Nanoscale

PAPER

View Article Online
View Journal | View Issue

Cite this: *Nanoscale*, 2016, **8**, 10406

Electrochemical activation of carbon cloth in aqueous inorganic salt solution for superior capacitive performance†

Dong Ye,[a] Yao Yu,*[a] Jie Tang,[b] Lin Liu[a] and Yue Wu[c]

Carbon cloth (CC) is an inexpensive and highly conductive textile with excellent mechanical flexibility and strength; it holds great promise as an electrode material for flexible supercapacitors. However, pristine CC has such a low surface area and poor electrochemical activity that the energy storage capability is usually very poor. Herein, we report a green method, two-step electrochemical activation in an aqueous solution of inorganic salts, to significantly enhance the capacitance of CC for supercapacitor application. Micro-cracks, exfoliated carbon fiber shells, and oxygen-containing functional groups (OFGs) were introduced onto the surface of the carbon filament. This resulted in an enhancement of over two orders of magnitude in capacitance compared to that of the bare CC electrode, reaching up to a maximum areal capacitance of 505.5 mF cm^{-2} at the current density of 6 mA cm^{-2} in aqueous H_2SO_4 electrolyte. Electrochemical reduction of CC electrodes led to the removal of most electrochemically unstable surface OFGs, resulting in superior charging/discharging rate capability and excellent cycling stability. Although the activated CC electrode contained a high-level of surface oxygen functional groups (~15 at %), it still exhibited a remarkable charging–discharging rate capability, retaining ~88% of the capacitance when the charging rate increased from 6 to 48 mA cm^{-2}. Moreover, the activated CC electrode exhibited excellent cycling stability with ~97% capacitance remaining after 10 000 cycles at a current density of 24 mA cm^{-2}. A symmetrical supercapacitor based on the activated CC exhibited an ideal capacitive behavior and fast charge–discharge properties. Such a simple, environment-friendly, and cost-effective strategy to activate CC shows great potential in the fabrication of high-performance flexible supercapacitors.

Received 22nd January 2016,
Accepted 15th April 2016

DOI: 10.1039/c6nr00606j

www.rsc.org/nanoscale

Introduction

Owing to the ever-increasing demands for renewable energy of modern societies, supercapacitors (SCs), a class of electrochemical energy storage devices, have drawn tremendous attention in applications of portable electronics, electric vehicles, and backup systems.[1–4] Carbon nanomaterials such as porous carbon materials,[1,5–8] carbon onions,[9] carbon nanotubes,[10,11] and graphene[12,13] are common choices of electrode materials due to their high conductivity, large surface area, chemical stability, and low cost. These electrodes exhibit some unique advantages such as high rate capabilities and long cycle lives due to their intrinsic operation mechanism, *e.g.* physical ion adsorption on a high surface area.[14] However, the specific capacitance is still not large enough as expected, which is attributed to the relatively low surface area available to charge storage from poor wettability. Introduction of doped heteroatoms or surface functional groups into carbon nanomaterials is one of the most efficient ways to solve the insufficient capacitance issue, as the heteroatoms or the surface oxygen groups in the carbon nanomaterials may improve the electrical conductivity and influence the wettability, consequently maximizing the electro-active surface area, or contributing to extra pseudocapacitance.[15–20]

Carbon cloth, a material consisting of carbon filaments about 5–10 μm in diameter, is a highly conductive textile with excellent mechanical flexibility, low weight, and chemical stability, showing great potential in the fabrication of flexible electrodes. However, because of its poor electrochemical activity, small specific surface area, and poor porosity, CC has

[a]*School of Materials Science and Engineering and State Key Lab for Materials Processing and Die and Mold Technology, Huazhong University of Science and Technology, 430074 Wuhan, China. E-mail: ensiyu@mail.hust.edu.cn; Tel: +8625 87556894*
[b]*1D Nanomaterials Group, NIMS, Sengen 1-2-1, Tsukuba 305-0047, Japan*
[c]*Department of Physics and Astronomy, University of North Carolina, Chapel Hill, NC 27599-3255, USA*
†Electronic supplementary information (ESI) available. See DOI: 10.1039/c6nr00606j

attracted very little attention for direct use as an electrode material except for current collectors or scaffolds for loading other capacitive materials. Recent research studies have shown that the surface area of a CC electrode can be significantly increased through controlled oxidative exfoliation of pristine carbon filaments as a result of the formed thin carbon fiber shell on the surface.[21,22] However, the energy storage capability is still not good enough (72 mF cm^{-2} at 6 mA cm^{-2} for CC) and mass production suffers from drawbacks from hazardous chemicals. By electrochemical activation of the CC in a H_2SO_4–HNO_3 mixture solution, a remarkable capacitance enhancement (756 mF cm^{-2} at 6 mA cm^{-2}) was also achieved because of the increased surface area and the introduced OFGs.[23] Such an areal capacitance is substantially higher than the values of recently reported carbon-based materials and some metal oxide anodes, such as CNT films (113 mF cm^{-2} at 5 mA cm^{-2}),[24] polypyrrole/graphene oxide nanocomposites (70.2 mF cm^{-2} at 5 mA cm^{-2}),[25] V_2O_5–PANI (421.5 mF cm^{-2} at 5 mA cm^{-2}),[26] and Ni/Co_3O_4 (410 mF cm^{-2} at 5.6 mA cm^{-2}).[27] Nevertheless, over half of the capacitance was lost when the charging rate increased from 6 to 40 mA cm^{-2}, which may originate from the slow Faraday reaction of some surface oxygen groups. Thus, the development of a new strategy to activate CC is still quite crucial for achieving superior energy storage and charging/discharging rate capabilities.

In this study, we report a facile and green activation strategy, electrochemical oxidative exfoliation followed by electrochemical reduction in an aqueous solution of inorganic salts, to introduce an oxygenated carbon fiber shell with some micro-cracks onto the surface of a carbon filament while preserving the mechanical properties of CC. Without loading other capacitive materials, the maximal areal capacitance of the activated CC electrode showed a 632-fold increase up to 505.5 mF cm^{-2} in 1.0 M aqueous H_2SO_4 electrolyte at a current density of 6 mA cm^{-2}. Electrochemical reduction can efficiently remove some unfavorable surface oxygen groups (*e.g.* carbonyl groups) and restore the conductivity of the CC electrodes.[28] Although the activated CC electrode contained a high-level of surface oxygen functional groups (~15 at%), it still exhibited a remarkable charging–discharging rate capability, retaining ~88% of the capacitance when the charging rate increased from 6 to 48 mA cm^{-2}. Moreover, the activated CC electrode exhibited excellent cycling stability with ~97% capacitance remaining after 10 000 cycles at a current density of 24 mA cm^{-2}. A symmetrical supercapacitor based on the activated CC exhibited an ideal capacitive behavior and fast charge–discharge properties. Activation of CC through such a facile, environment-friendly, and cost-effective method offers new opportunities in the fabrication of high-performance flexible SCs.

Experimental section

All chemicals were of analytical grade and used as received without further purification.

Electrochemical activation of carbon cloth

The activated CC was obtained by an electrochemical oxidative exfoliation followed by electrochemical reduction. Before activation, a piece of carbon fiber cloth (~1 × 1 cm, mass per unit area 12 mg cm^{-2}, 0.32 mm in thickness, from CeTech, Taiwan) was cleaned with an alcohol and acetone mixture solution (v : v = 1 : 1), and deionized water twice in turn. The electrochemical oxidative exfoliation was carried out in a standard two-electrode system in 100 mL 0.1 M $(NH_4)_2SO_4$ aqueous solution using platinum as the cathode and a piece of carbon fiber cloth as the anode. A direct current voltage of +10 V was applied to the anode with a processing time of 5, 10, 15, 20, and 25 min for each, neglecting the water splitting (denoted as OCC-*X*, *X* represents the treatment duration in minutes). The electrochemical reduction was carried out in a three-electrode system with 50 mL 1.0 M NH_4Cl aqueous solution as the electrolyte, in which a platinum plate electrode was employed as the counter electrode, an Ag/AgCl electrode worked as the reference electrode, and the OCC-*X* was directly used as the working electrode. All these electrodes were reduced under potentiostatic polarization at −1.2 V for 30 min at room temperature (denoted as ECC-*X*, *X* represents the treatment duration in minutes). ECCs were washed with deionized water and kept in pure water for further use.

Material characterization

The overall appearance and morphologies of the carbon fiber cloth were characterized using field emission scanning electron microscopy (SEM, FEI Sirion 200) and transmission electron microscopy (TEM, Tecnai G2 20). The functional group distribution was characterized by using X-ray photoelectron spectroscopy (XPS, Kratos, and AXIS ULTRA DLD-600W), Fourier transform infrared spectroscopy (FT-IR, VERTEX 70), and Raman spectroscopy (Raman, LabRAM HR800). Ultraviolet-visible spectroscopy (UV-vis, Lambda 35) was carried out to detect the concentration of methylene blue aqueous solution. Brunauer–Emmett–Teller (BET, Micromeritics ASAP 2020) analysis was carried out to measure the surface area of samples.

Electrochemical evaluation

For a three-electrode system, a small piece of related CC with a surface area of 1.0 cm^2 (1 cm × 1 cm) was used exclusively as the working electrode. Ag/AgCl (saturated KCl solution) and a Pt plate were used as the reference and counter electrodes, respectively. Cyclic voltammetry and galvanostatic charge–discharge were performed over the potential range of −0.2–0.8 V, and electrochemical impedance spectroscopy was carried out between 10 k and 0.1 Hz with a potential perturbation of 10 mV, with 1.0 M H_2SO_4 as the electrolyte solution. For supercapacitor tests, two ECC-15 electrodes with the same area were connected to two platinum wires as working electrodes, and the test was carried out in a two-electrode system. The electrodes were first attached to glass slides, and both the glass slides were assembled with a filter paper sandwiched in between.

Then the cell assemblies were dipped in 1.0 M H_2SO_4 electrolyte. Cyclic voltammetry (CV) and galvanostatic charge–discharge (GCD) were performed over the potential range of 0–1 V, and electrochemical impedance spectroscopy was carried out under open-circuit voltage from a frequency of 10 k to 0.1 Hz. All the tests were performed using a PARSTAT 4000 electrochemical workstation (Princeton Applied Research).

Calculation

Specific areal capacitances of carbon cloth electrodes were calculated from their cyclic voltammograms according to the following equation: $C_s = \frac{Q_{ave}}{V \cdot S}$, where C_s is the specific areal capacitance with the unit of F cm^{-2}, Q_{ave} is the average charge with the unit of coulomb during the charging and discharging process, V is the potential window with the unit of volt, and S is the projected area of the carbon cloth with the unit of square centimeters. Alternatively, the specific areal capacitances of electrodes were measured using the galvanostatic charging–discharging method based on the following equation: $C_s = \frac{I \cdot \Delta t}{\Delta V \cdot S}$, where I is the constant discharging current, Δt is the discharging time, and ΔV is the potential difference with consideration of the IR drop (I = current, R = resistance).

Results and discussion

Motivated by the previous studies on electrochemical exfoliation of graphite into graphene[29–31] and electrochemical reduction of graphene oxide,[28,32] our strategy for the activation of CC involves two steps: electrochemical oxidative exfoliation and electrochemical reduction in aqueous solution of inorganic salts, as shown in Scheme 1 (see details in the Experimental section). Electrochemical oxidative exfoliation of CC was performed in a two-electrode system in 0.1 M $(NH_4)_2SO_4$ aqueous solution taking a platinum plate as the cathode and a piece of CC as the anode. A series of measurements was taken when a direct current voltage of +10 V was applied to the CC electrodes for the desired processing time. As the generated OFGs deteriorated the electrical conductivity of a single carbon filament and increased the contact resistance between the filaments, the square resistance of the CC electrodes increased rapidly from ten ohms to dozens of kilohms. Previous studies have shown that an insulating graphene oxide hydrogel film can be electrochemically reduced in 1.0 M NH_4Cl aqueous solution by using a three-electrode system while the film is brought into contact with an Ag wire by a multi-line contact, and this served as the working electrode.[32] Though the insulating film isn't fully in contact with the Ag wire, the whole film is still reduced by optimizing the processing time. Inspired by

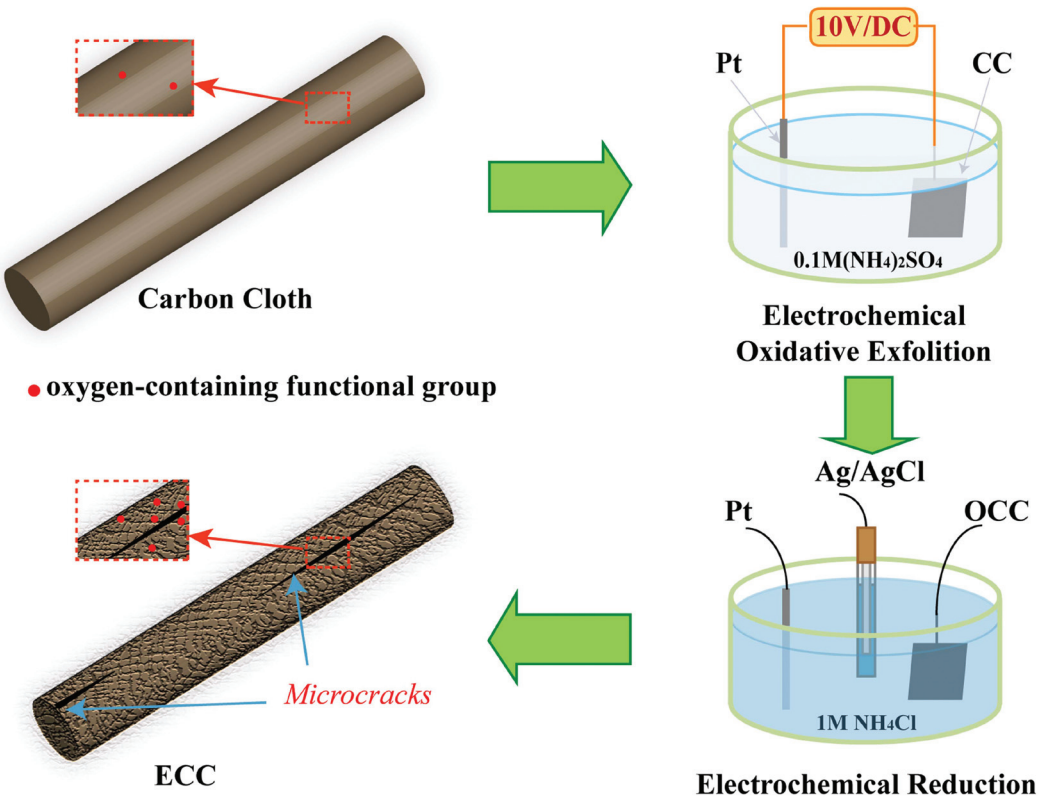

Scheme 1 Schematic diagram illustration of *in situ* electrochemical activation of the carbon fiber cloth in aqueous solution of 0.1 M $(NH_4)_2SO_4$ and electrochemical reduction of this oxidized carbon fiber cloth in aqueous solution of 1.0 M NH_4Cl.

this approach, by directly taking the OCC-*X* samples as the working electrode, we carried out the electrochemical reduction process in 1.0 M NH_4Cl aqueous solution under the three-electrode system by potentiostatic polarization at −1.2 V.[28,32–35] As the high diffusion of electrons can diffuse anywhere the electrolyte exists, the electrochemical reactions between the electrons and the surface OFGs are efficient. The ECC-*X* electrodes with a square resistance of several dozens of ohms could be obtained after 30 min of reduction. The ECC-*X* electrodes preserved the good flexibility (similar to ECC-15 in Fig. S1†), and further electrochemical energy storage capability tests indicated that the optimal performance was achieved at 15 min of electrochemical oxidative exfoliation. SEM reveals that the pristine CC consists of interlaced carbon filaments with a smooth surface (Fig. 1a–c). After electrochemical activation, the surface of carbon filaments became relatively rough with a number of nano-channels, a typical sign of oxidative exfoliation.[21–23,29] And some micro-cracks were formed at the same time (Fig. 1d, red arrows), which may originate from the gaseous species such as SO_2 and O_2 evolution inside the initial nano-cracks during the electrochemical process (Fig. 1d–f).[30,31] To further examine their modified surface, the ECC-15 sample was characterized by TEM (Fig. 1f and g). Fig. 1e clearly reveals the formation of core–shell shaped carbon filaments with a shell of ~100 nm in thickness. The high resolution TEM image and selected area electron diffraction pattern both show the signature of the fully amorphous structure of the well-exfoliated carbon fiber shell (Fig. 1f).

To test our hypothesis of the enhancement in the effective electrode surface area through electrochemical exfoliation, we investigated the variation of the surface area of pristine CC and ECC-15 electrodes using the dye-adsorption method.[22] Methylene blue (MB) is a widely chosen dye to determine the surface area of a solid adsorber. The pristine CC and ECC-15 electrodes (sizes: 1 cm × 1 cm) were soaked in 50 mL of 2 mg L^{-1} MB aqueous solution under constant stirring in the dark, respectively. After 16 hours, the MB solution with the ECC-15 electrode became colorless while that with the pristine CC sample remained blue as the original MB solution, suggesting that a significant portion of dye molecules was adsorbed onto the activated sample (Fig. 2a, inset). Moreover, the UV-vis absorption spectra (Fig. 2a) collected from these solutions reveal an obviously decreased MB intensity (665 nm) with the ECC-15 sample. This indicates that more MB dye molecules were adsorbed on the activated sample than the pristine sample, confirming the enhanced ion accessible surface area in the ECC-15 sample. Further nitrogen adsorption–desorption isotherm analysis reveals that the specific surface area is increased from 0.4 m^2 g^{-1} for CC to 14.3 m^2 g^{-1} for ECC-15 (the averaged pore size is estimated to be about 200 nm), which agrees with the dye-adsorption results. These results are consistent with the SEM and TEM results, and it supports the fact that the surface area of the activated CC was substantially

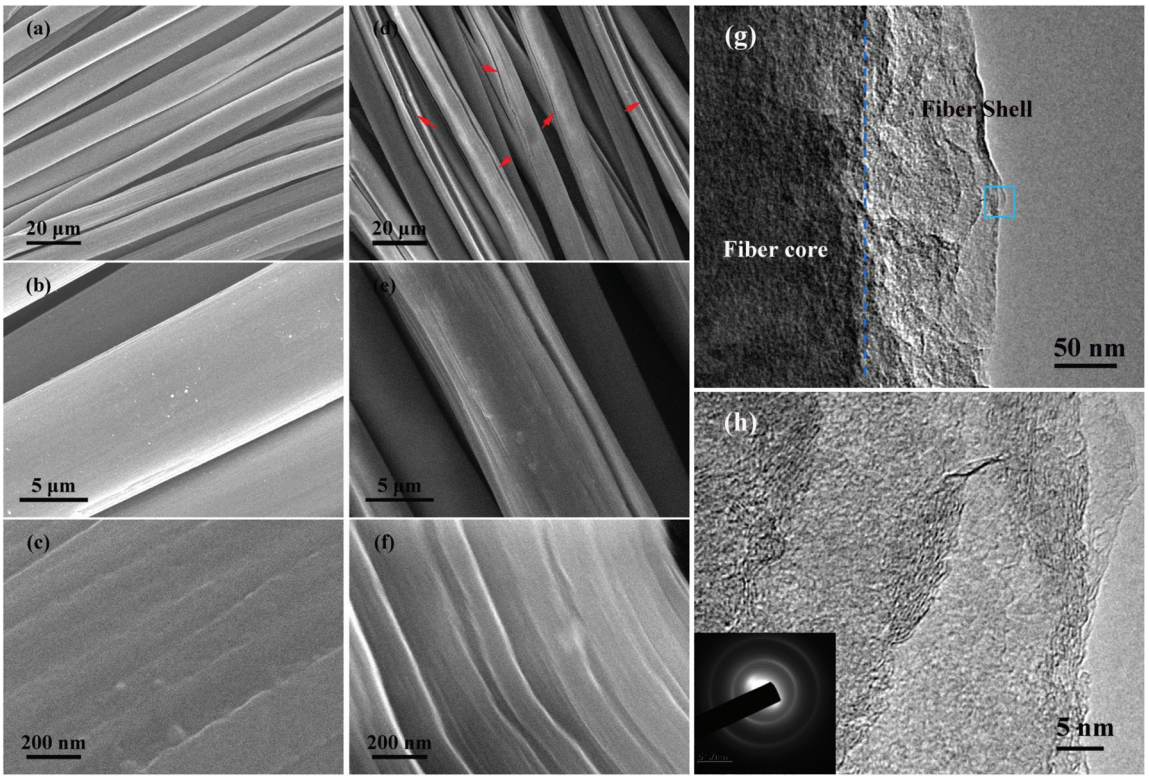

Fig. 1 SEM images of carbon filaments in pristine carbon cloth (a), (b), (c) and ECC-15 (d), (e), (f); (g) TEM image of ECC-15 and (h) high-resolution TEM image corresponding to the square area in (g), the inset shows the selected area electron diffraction pattern of ECC-15.

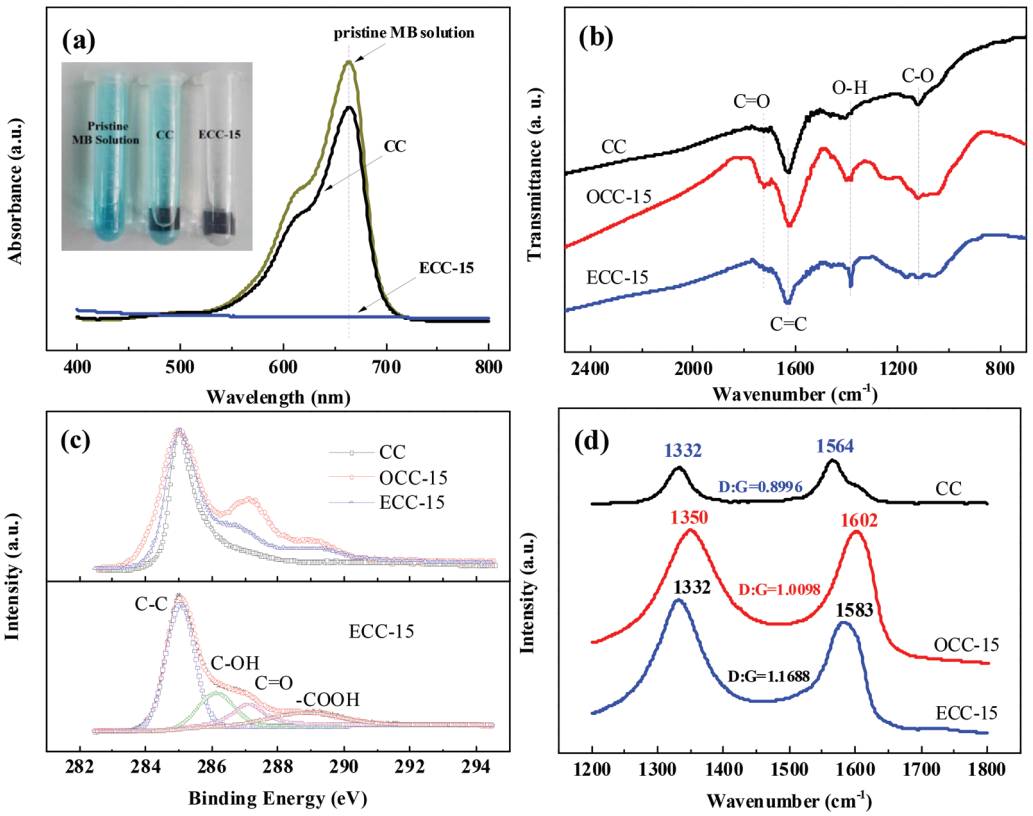

Fig. 2 (a) UV-vis absorption spectra collected for the pristine MB solution (2 mg L^{-1} in water) and for the MB solutions after reacting with pristine CC, and ECC-15 for 16 h. The inset photograph is a digital image of these solutions; FT-IR spectra (b), high-resolution C_{1s} XPS spectra (c), and Raman spectra (d) of pristine CC, OCC-15, and ECC-15, respectively.

increased by the two-step electrochemical treatment in salt aqueous solution.

In order to confirm the oxidative activation, the pristine CC, OCC-15, and ECC-15 samples were further characterized by FT-IR, XPS and Raman spectroscopy. The FT-IR spectra show that there is an obvious enhancement of the band centered at ~1730 cm^{-1} and ~1120 cm^{-1} in the OCC-15 sample compared to the pristine CC electrode (Fig. 2b), indicating the formation of hydroxyl and carboxyl groups on the CC surface.[36] The oxygen content in OCC-15 is 24.3 at%, about five times larger than that of the pristine CC (4.6 at%). And its high resolution C_{1s} spectrum has a broader signal than the untreated sample, showing the existence of other chemical states of carbon on the surface (Fig. 2c, upper). Application of the bias voltage (DC, +10 V) can result in the reduction of water at the cathode, creating hydroxyl ions (OH^-) that act as a strong nucleophile in the electrolyte. Due to the nucleophilic attack of CC by OH^-, active site atoms on the filament surface could be oxidized to form such OFGs as C–OH, C═O, and COOH, and this is the reason for the deterioration of electrical conductivity. The oxygen content of ECC-15 is 14.8 at%, which is much lower than OCC-15 but is still higher than the pristine CC.[30,37] The C_{1s} XPS spectrum of ECC-15 can be deconvoluted into four peaks assigned to C–C (285.0 eV), C–OH (286.1 eV), C═O (287.1 eV), and –COOH (288.8 eV) groups, respectively (Fig. 2c, lower).[23,38] These peaks reveal that there are still many residual OFGs on the surface, though the electrical conductivity is restored apparently in ECC-15. The Raman spectra show that the G bands of both OCC-15 and ECC-15 samples were broadened and exhibited some upshift compared to the pristine CC (Fig. 2d). Besides, the D bands also became prominent, indicating the reduction in the size of the in-plane sp^2 domains. These features indicate a larger disorder degree on the surface of the activated CC samples, possibly due to the introduced OFGs and surface etching. The increase in the I_D/I_G ratio from 1.0098 to 1.1688 suggests a decrease in the average size of the sp^2 domain on the surface of the ECC-15 sample, suggesting that many new sp^2 graphite domains were created that are smaller in size than the ones present on the surface of OCC-15. This indicates that the disorder degree reduced at some local site on the surface of ECC-15 due to the partial removal of OFGs, confirming the real reduction of OCC-15 as well.[28,32] Similar to the electrochemical reduction of the graphene oxide hydrogel film, the negative potential could overcome the energy barriers and the OFGs on the surface of OCC-15 can be reduced. And the electrochemical reactions between the electrons and the OFGs are efficient because the electrolyte can diffuse throughout the OCC-15 electrode.

The electrochemical performances of the pristine CC, OCC-15 and ECC-15 samples were first investigated using a

three-electrode system in 1.0 M H_2SO_4 aqueous electrolyte. As can be seen in Fig. 3a, the ECC-15 electrode produces a non-rectangular shape of the CV curve with a pair of redox peaks around 0.2 V and 0.5 V, suggesting the existence of pseudo-capacitance of the ECC-15 electrode due to the surface residual functional groups.[39,40] And its curve exhibits an area two orders of magnitude larger than that of the pristine CC and OCC-15 electrodes at the scan rate of 20 mV s^{-1}, showing a substantially enhanced charge storage capability of the ECC-15 electrode. The OCC-15 electrode shows several times larger current density than that of the untreated CC electrodes; however, it is still about an order of magnitude less than that of the ECC-15 electrode. The slight increase in capacitive of the OCC-15 electrode should be attributed to the increased surface area and the introduced OFGs, while too many OFGs result in a relatively low capacitance because of its low conductivity.[32–35] Further GCD tests as shown in Fig. 3b show similar results as well. The ECC-15 electrode exhibits a symmetrical triangle shaped curve with a much longer discharge time than that of the pristine CC and OCC-15 electrodes. The enhancement in capacitance of the ECC-15 compared with OCC-15 should be attributed to the significantly improved electrical conductivity, where similar effects occur in the electrochemical reduction of graphene oxide.[32,35] These characteristics confirmed the successful activation of the CC electrodes and demonstrated that the reduction step is crucially essential for such efficient electrochemical activation, the reason for which can also be concluded from EIS analyses. Among the three electrodes, the vertical curve of the pristine CC electrode has the largest slope with respect to the real impedance axis (Z_{re}) in Nyquist plots (Fig. 3c), implying the highest conductivity or lowest internal resistance nature of the pristine CC electrode. In contrast, the low-frequency Nyquist plot of the OCC-15 electrode shows the typical Warburg impedance characteristic, where the electrochemical reaction mechanism is dominated by the ion diffusion effects at the electrolyte/electrode interfaces, indicating that the abundance of the introduced OFGs decreased the ion transport at the electrode–electrolyte interface. These groups also induce a rather high charge transfer resistance (~5.0 Ω, the diameter of the incomplete semicircle as shown in Fig. 3c inset), eventually causing the low charge storage capability of the OCC-15 electrode. Fortunately, the redundant surface functional groups can be removed off the carbon filament through the electrochemical reduction process, leaving an ECC-15 electrode with low Warburg impedance and charge transfer resistance (~0.8 Ω). The slight increase in the series resistance (the intersection point on the Z_{re} axis) from 1.5 Ω of the pristine CC to 2.1 Ω of the ECC-15 electrode suggests that the electrochemical activation has caused subtle deterioration in the internal conductivity of the CC electrode.

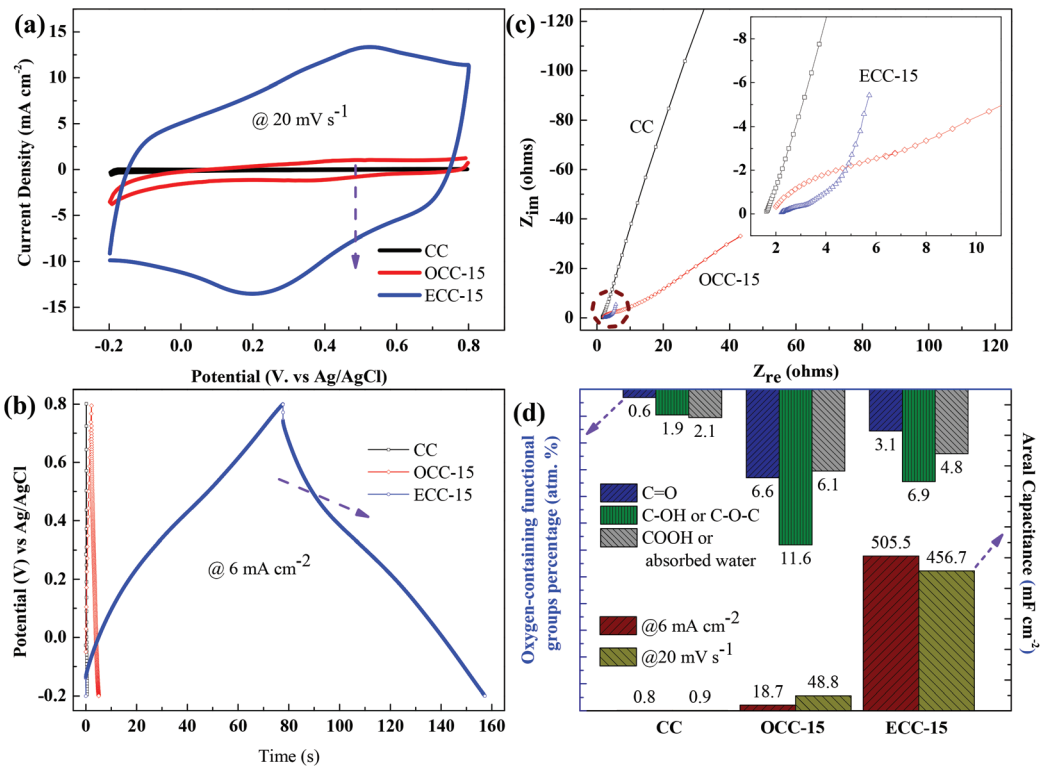

Fig. 3 CV curves collected at the scan rate of 20 mV s^{-1} (a), GCD curves collected at a current density of 6 mA cm^{-2} (b), and Nyquist plot (c) from the pristine CC, OCC-15, and ECC-15 as the working electrodes in 1.0 M aqueous H_2SO_4 electrolyte in a three-electrode configuration; (d) areal capacitance (calculated from both the CV curve at the scan rate of 20 mV s^{-1} and the GCD curve at the current density of 6 mA cm^{-2}) and the content of oxygen-containing functional groups of the corresponding electrodes.

Fig. 3d shows the areal capacitance, which is calculated from both the CV curve at the scan rate of 20 mV s^{-1} and the GCD curve at the current density of 6 mA cm^{-2}, and the content of OFGs based on the O 1s XPS spectrum of the corresponding CC, OCC-15, and ECC-15 electrodes (seen in Fig. S2†). The electrochemical oxidative exfoliation step induces the surface exfoliation of the carbon filaments and the introduction of tremendous OFGs onto the surface of CC, leading to the increase in the content of C═O, C–OH or C–O–C, and C(O)OH on the surface of CC from 0.6 at%, 1.9 at%, 2.1 at% to 6.6 at%, 11.6 at%, and 6.1 at%, respectively. Such a high content of OFGs surely will contribute much more pseudocapacitance; however, the conductivity of the OCC-15 electrode is so poor that it could not exhibit a high capacitance as expected. After carrying out electrochemical reduction process, some unstable OFGs were removed off the surface of the OCC-15 electrode, resulting in significant improvement in its electrical conductivity. As we expected, most of the unfavorable surface carbonyl groups are removed, the content of which decreases from 6.6 at% to 3.1 at%; while the hydroxyl and carboxyl groups that can contribute to an extra reversible pseudocapacitance are furthest maintained, the whole content of which is about 11.7 at%.[23] The slightly increased surface area along with the oxygenated carbon fiber shell with balanced OFGs and conductivity lead to the significant enhancement in the charge storage capability of the ECC-15 electrode, reaching up to a maximum areal capacitance of 505.5 mF cm^{-2} at the current density of 6 mA cm^{-2} in aqueous H_2SO_4 electrolyte. A further study as

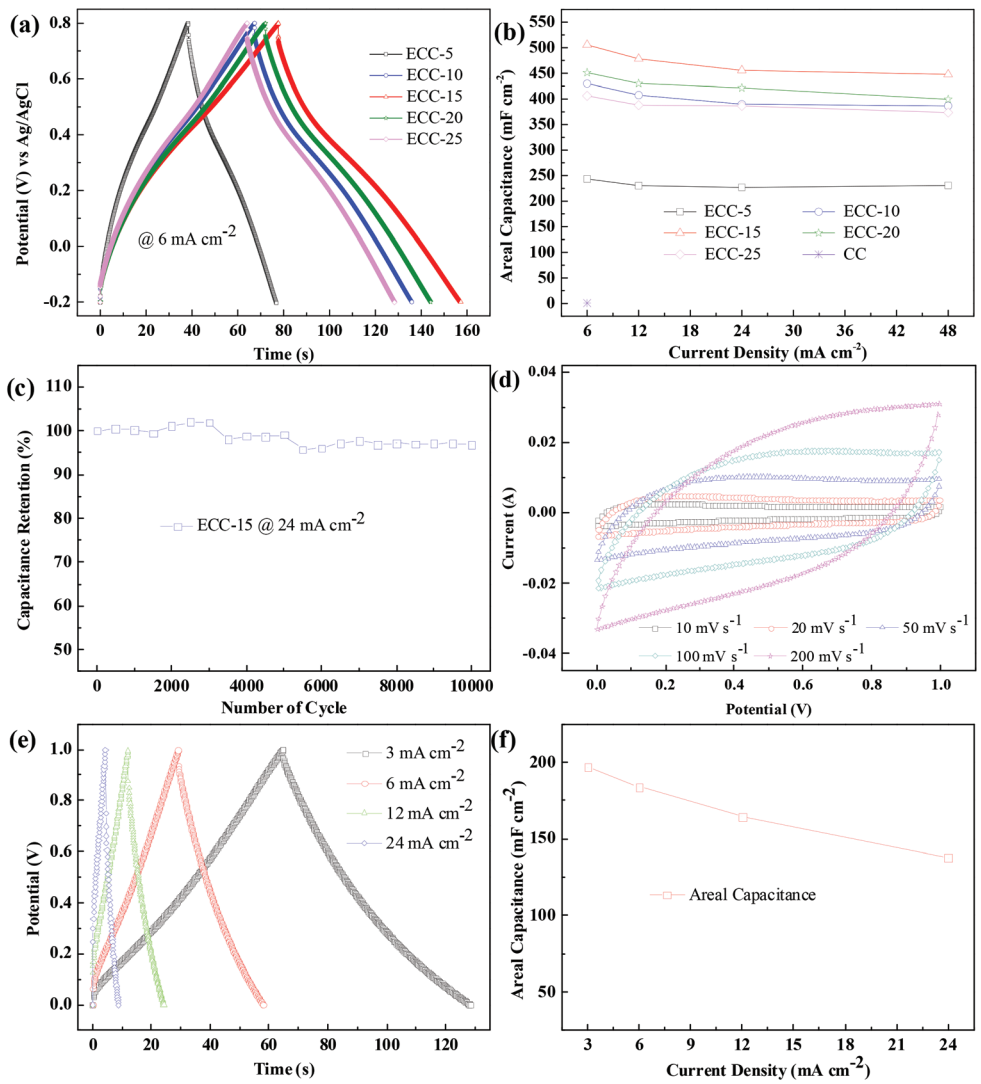

Fig. 4 GCD curves of the activated CC electrodes collected at a current density of 6 mA cm^{-2} as a function of exfoliation time (a) and the corresponding rate capability of these electrodes at a current density from 6 mA cm^{-2} to 48 mA cm^{-2} (b); cyclic stability of the ECC-15 electrodes collected at 24 mA cm^{-2} for 10 000 cycles (c); all the tests were carried out in 1.0 M aqueous H_2SO_4 electrolyte in a three-electrode configuration. CV curves collected at the scan rate from 10 mV s^{-1} to 200 mV s^{-1} (d), GCD curves collected at a current density from 3 mA cm^{-2} to 24 mA cm^{-2} (e) from ECC-15 as the working electrodes in 1.0 M aqueous H_2SO_4 electrolyte in a two-electrode configuration; (f) areal capacitance as a function of the current density of the supercapacitor.

follows shows that it exhibits a remarkable charging–discharging rate capability as well.

The effect of the activation time on the capacitive performance of CC electrodes was also studied. Fig. 4a shows that all GCD curves exhibit a symmetrical triangle shape with a slight distortion, suggesting excellent reversibility of the pseudocapacitance. The discharge time gradually increased with the activation time from 5 to 15 min at a low current density of 6 mA cm^{-2}, while both the series resistance and charge transfer resistance show little changes (Fig. S3†), indicating that the substantially increased surface functional groups are helpful for enhancing the pseudocapacitance. However, the ECC electrodes exhibited a decreased discharge time, and an increased series resistance and charge transfer resistance when the activation time is over 15 min, showing that excessive functional groups will lead to an inferior electrode/electrolyte interface.[23] Nevertheless, there is little differences among the CV curves of samples with an activation time over 10 min collected at a higher scan rate of 100 mV s^{-1} (seen in Fig. S4†), maybe due to the slow redox reaction of the introduced OFGs that could not keep pace with such a high scan rate. Fig. 4b plots the areal capacitance of the activated electrodes as a function of oxidative exfoliation time. All the activated electrodes processed a prominent rate capability with more than 88% retention of its initial capacitance as the current density increased from 6 to 48 mA cm^{-2}. The ECC-15 electrode achieves a high areal capacitance of 505.5 mF cm^{-2} at the current density of 6 mA cm^{-2} (~15.8 F cm^{-3}, seen in Table S1†) and exhibits excellent cycling stability with ~97% capacitance remaining after 10 000 cycles at a high charging rate of 24 mA cm^{-2}. The areal capacitance of the ECC-*X* (*X* is not less than 10) electrodes was calculated from the CV curves at a high scan rate of 100 mV s^{-1} to be around 300 mF cm^{-2} (seen in Fig. S5†), the value of which is higher than 208.9 mF cm^{-2} of the previous similar study.[23] Electrochemical reduction of CC electrodes induced the removal of most electrochemically unstable OFGs and the restoration of the electrode conductivity, resulting in the above superior electrochemical performances. To estimate the feasibility of the activated CC as electrode materials, two pieces of the ECC-15 electrodes are directly assembled with a filter paper sandwiched in between for the symmetrical supercapacitor test. Fig. 4e, and f show the corresponding CV and GCD curves of the device collected at various scan rates and current densities, respectively. The rectangular-like CV curves and symmetric triangular charge/discharge curves show the ideal capacitive behavior and fast charge–discharge properties of the activated CC based supercapacitor. Fig. 4g shows the areal capacitance of the symmetrical device as a function of current density, and the device delivered a maximum areal capacitance of 197 mF cm^{-2} at a current density of 3 mA cm^{-2}.

Conclusions

In conclusion, we presented a green and facile approach to significantly enhance the capacitance of pure CC for supercapacitor applications. Through electrochemical oxidative exfoliation followed by electrochemical reduction in an aqueous solution of inorganic salts, micro-cracks, exfoliated carbon fiber shells, and OFGs are introduced onto the surface of a carbon filament while preserving its flexibility. This results in an enhancement of over two orders of magnitude in capacitance compared to that of the bare CC, reaching up to a maximum areal capacitance of 505.5 mF cm^{-2} at the current density of 6 mA cm^{-2} in aqueous H_2SO_4 electrolyte measured in a three-electrode cell. More importantly, it exhibits a remarkable charging–discharging rate capability, retaining 88% of the capacitance when the charging rate increased from 6 to 48 mA cm^{-2}. Moreover, the electrode shows excellent cycling stability with ~97% capacitance remaining after 10 000 cycles at a charging rate of 24 mA cm^{-2}. A symmetrical supercapacitor based on the activated CC exhibits an ideal capacitive behavior and fast charge–discharge properties, and delivers a maximum areal capacitance of 197 mF cm^{-2} at 3 mA cm^{-2}. This simple, environment-friendly, and cost-effective strategy to activate CC shows great potential in the development of high-performance electrode materials for flexible supercapacitors.

Acknowledgements

This work was financially supported by the National Natural Science Foundation of China (Grant No. 51402119) and the special foundation for the National Thousands Talent Program in Huazhong University of Science and Technology (HUST). The authors are grateful to the Analytical and Testing Center of HUST for technical assistance.

References

1 L. L. Zhang and X. S. Zhao, *Chem. Soc. Rev.*, 2009, **38**, 2520–2531.
2 J. M. Miller, B. Dunn, T. D. Tran and R. W. Pekala, *J. Electrochem. Soc.*, 1997, **144**, L309–L311.
3 E. Frackowiak and F. Beguin, *Carbon*, 2001, **39**, 937–950.
4 J. R. Miller and P. Simon, *Science*, 2008, **321**, 651–652.
5 D. Y. Qu and H. Shi, *J. Power Sources*, 1998, **74**, 99–107.
6 C. Merlet, B. Rotenberg, P. A. Madden, P. L. Taberna, P. Simon, Y. Gogotsi and M. Salanne, *Nat. Mater.*, 2012, **11**, 306–310.
7 Q. Cheng, J. Tang, J. Ma, H. Zhang, N. Shinya and L. C. Qin, *J. Phys. Chem. C*, 2011, **115**, 23584–23590.
8 T. C. Zhang, C. H. J. Kim, Y. W. Cheng, Y. W. Ma, H. B. Zhang and J. Liu, *Nanoscale*, 2015, **7**, 3285–3291.
9 D. Pech, M. Brunet, H. Durou, P. H. Huang, V. Mochalin, Y. Gogotsi, P. L. Taberna and P. Simon, *Nat. Nanotechnol.*, 2010, **5**, 651–654.
10 L. B. Hu, D. S. Hecht and G. Gruner, *Chem. Rev.*, 2010, **110**, 5790–5844.
11 D. S. Yu, K. Goh, H. Wang, L. Wei, W. C. Jiang, Q. Zhang, L. M. Dai and Y. Chen, *Nat. Nanotechnol.*, 2014, **9**, 555–562.

12 F. Beguin, V. Presser, A. Balducci and E. Frackowiak, *Adv. Mater.*, 2014, **26**, 2219–2251.
13 M. D. Stoller, S. J. Park, Y. W. Zhu, J. H. An and R. S. Ruoff, *Nano Lett.*, 2008, **8**, 3498–3502.
14 B. E. Conway, Electrochemical supercapacitors: scientific fundamentals and technological application, 1999.
15 Z. S. Wu, A. Winter, L. Chen, Y. Sun, A. Turchanin, X. L. Feng and K. Mullen, *Adv. Mater.*, 2012, **24**, 5130–5135.
16 S. Maldonado, S. Morin and K. J. Stevenson, *Carbon*, 2006, **44**, 1429–1437.
17 X. R. Wang, X. L. Li, L. Zhang, Y. Yoon, P. K. Weber, H. L. Wang, J. Guo and H. J. Dai, *Science*, 2009, **324**, 768–771.
18 H. M. Jeong, J. W. Lee, W. H. Shin, Y. J. Choi, H. J. Shin, J. K. Kang and J. W. Choi, *Nano Lett.*, 2011, **11**, 2472–2477.
19 X. W. Wang, G. Z. Sun, P. Routh, D. H. Kim, W. Huang and P. Chen, *Chem. Soc. Rev.*, 2014, **43**, 7067–7098.
20 D. Ye, S. Q. Wu, Y. Yu, L. Liu, X. P. Lu and Y. Wu, *Appl. Phys. Lett.*, 2014, **104**, 103105.
21 D. Yu, S. Zhai, W. Jiang, K. Goh, L. Wei, X. Chen, R. Jiang and Y. Chen, *Adv. Mater.*, 2015, **27**(33), 4895–4901.
22 G. M. Wang, H. Y. Wang, X. H. Lu, Y. C. Ling, M. H. Yu, T. Zhai, Y. X. Tong and Y. Li, *Adv. Mater.*, 2014, **26**, 2676–2682.
23 W. Wang, W. Y. Liu, Y. X. Zeng, Y. Han, M. H. Yu, X. H. Lu and Y. X. Tong, *Adv. Mater.*, 2015, **27**, 3572–3578.
24 B. Yao, L. Y. Yuan, X. Xiao, J. Zhang, Y. Y. Qi, J. Zhou, J. Zhou, B. Hu and W. Chen, *Nano Energy*, 2013, **2**, 1071–1078.
25 H. H. Zhou, G. Y. Han, Y. M. Xiao, Y. Z. Chang and H. J. Zhai, *J. Power Sources*, 2014, **263**, 259–267.
26 M. H. Bai, T. Y. Liu, F. Luan, Y. Li and X. X. Liu, *J. Mater. Chem. A*, 2014, **2**, 10882–10888.
27 D. L. Chao, X. H. Xia, C. R. Zhu, J. Wang, J. L. Uu, J. Y. Lin, Z. X. Shen and H. J. Fan, *Nanoscale*, 2014, **6**, 5691–5697.
28 H. L. Guo, X. F. Wang, Q. Y. Qian, F. B. Wang and X. H. Xia, *ACS Nano*, 2009, **3**, 2653–2659.
29 C. T. J. Low, F. C. Walsh, M. H. Chakrabarti, M. A. Hashim and M. A. Hussain, *Carbon*, 2013, **54**, 1–21.
30 K. Parvez, Z. S. Wu, R. J. Li, X. J. Liu, R. Graf, X. L. Feng and K. Mullen, *J. Am. Chem. Soc.*, 2014, **136**, 6083–6091.
31 C. Y. Su, A. Y. Lu, Y. P. Xu, F. R. Chen, A. N. Khlobystov and L. J. Li, *ACS Nano*, 2011, **5**, 2332–2339.
32 X. Y. Feng, W. F. Chen and L. F. Yan, *Nanoscale*, 2015, **7**, 3712–3718.
33 Nicholas, A. Kotov, I. Dékány and J. H. Fendler, *Adv. Mater.*, 1996, **8**, 637–641.
34 M. Zhou, Y. L. Wang, Y. M. Zhai, J. F. Zhai, W. Ren, F. A. Wang and S. J. Dong, *Chem. – Eur. J.*, 2009, **15**, 6116–6120.
35 Y. Y. Shao, J. Wang, M. Engelhard, C. M. Wang and Y. H. Lin, *J. Mater. Chem.*, 2010, **20**, 743–748.
36 A. J. L.-P. C. Hontoria-Lucas, J. de D. López-González, M. L. Rojas-Cervantes and R. M. Martín-Aranda, *Carbon*, 1995, **33**, 1585–1592.
37 Z. R. Yue, W. Jiang, L. Wang, S. D. Gardner and C. U. Pittman, *Carbon*, 1999, **37**, 1785–1796.
38 X. Z. Fan, Y. H. Lu, H. B. Xu, X. F. Kong and J. Wang, *J. Mater. Chem.*, 2011, **21**, 18753–18760.
39 M. Seredych, D. Hulicova-Jurcakova, G. Q. Lu and T. J. Bandosz, *Carbon*, 2008, **46**, 1475–1488.
40 D. Hulicova-Jurcakova, M. Seredych, G. Q. Lu and T. J. Bandosz, *Adv. Funct. Mater.*, 2009, **19**, 438–447.